Electrochemistry

Received: November 20, 2015
Accepted: February 4, 2016
Published: May 5, 2016

The Electrochemical Society of Japan

http://dx.doi.org/10.5796/electrochemistry.84.338

Article

Electrochemistry, **84(5)**, 338–341 (2016)

Hairpin DNA Unzipping Analysis Using a Biological Nanopore Array

Masayuki OHARA, Yusuke SEKIYA, and Ryuji KAWANO*

Department of Life Science and Biotechnology, Tokyo University of Agriculture and Technology, 2-24-16 Naka-cho, Koganei, Tokyo 184-8588, Japan

* *Corresponding author: rjkawano@cc.tuat.ac.jp*

ABSTRACT

This paper describes a method of hairpin DNA (hpDNA) unzipping analysis using a biological nanopore array. Various lengths of hpDNAs were captured and translocated through the nanopore and the individual duration times were monitored. The correlation between the unzipping time and the simulated hybridization energy of the duplexes was able to be modeled as first-ordered reaction. This method is one of the approach for understanding of basic biological reactions in DNA replication and RNA transcription.

Keywords : Nanopore, DNA Unzipping, Lipid Bilayer

1. Introduction

Nanopore measurement is a powerful tool for single-molecule analysis. A pore-forming protein, α-hemolysin (αHL) is a popular biological nanopore, is reconstituted in a lipid bilayer, and the channel current through the αHL nanopore can be measured using a patch-clamp amplifier.[1,2] When a single molecule translocates through the nanopore electrophoretically, the blocking current is clearly observed because the ion flowing is prevented.[3] Blocking currents enable the electrical identification of distinct molecular configurations and the elucidation of mechanisms responsible for single molecule behavior, such as single molecule transport,[4] protein unfolding,[5] and DNA unzipping.[6] Therefore, this method has been attracting attention as a next-generation of DNA sequencing or a single-molecule detection technique.[7]

The unzipping behavior of double-stranded DNA (dsDNA) is important in many cellular processes, such as DNA replication and RNA transcription. The forces and timescales associated with the breakage of DNA/RNA strands have been studied at the single-molecule level.[8] The single DNA unzipping behavior has also been studied through nanopore measurement using the αHL pore.[9–11] The αHL pore, which consists of a vestibule (2.5 nm diameter) and a cylindrical pore (1.5 nm diameter) as shown in Fig. 1, is suitable for the dsDNA unzipping analysis. While ssDNA can pass through the entire αHL pore, dsDNA can get obstructed in the 2.5 nm vestibule section (Fig. 1a). The clogged dsDNA is unzipped and translocated within the nanopore, and the sequence-dependent duration time at single-molecule levels can be measured (Fig. 1b). In this experiment, a massive data set is needed for the stochastic analysis.

We recently proposed a multiple planar lipid bilayer system using microdroplets, named as a "droplet contact method" (DCM). A planar lipid bilayer can spontaneously form at the interface between the contacting microdroplets in an oil/lipid mixture solution (Fig. 2a). In this method, membrane stability, which usually remains for >300 h, is improved by reducing the contact area.[12] Furthermore, we constructed a droplet array for high-throughput measurements.[13] Using bilayer lipid membranes (BLMs), we measured various membrane proteins and biological nanopore, for example, single molecule detection using DNA aptamers,[14] high-throughput ion channel measurements at the single-protein level,[13,15,16] solution-exchange techniques via the microdroplet system,[17] and the development of portable nanopore sensors.[18] In this study, we

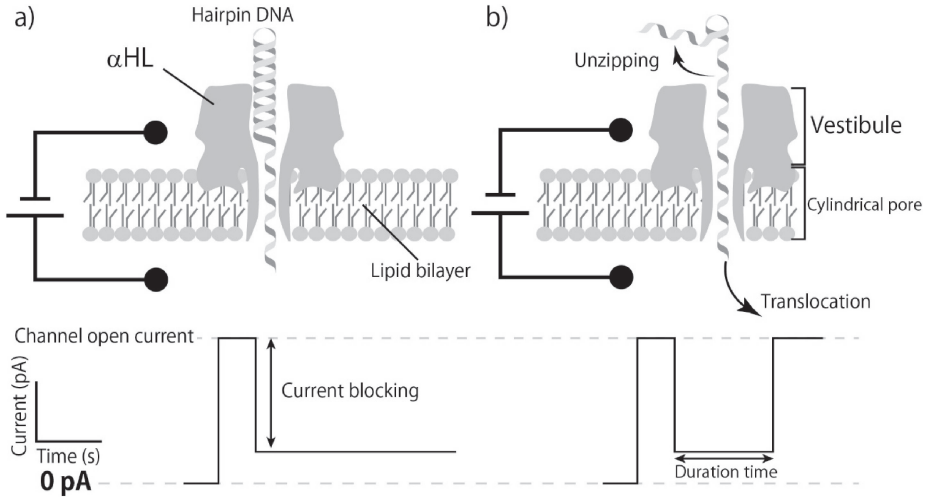

Figure 1. Schematic diagrams of hpDNA unzipping in the αHL nanopore. a) When hpDNA was clogged in the pore, the current signal decreased with long duration times (bottom trace). b) When hpDNA was unzipped under applied voltage at 120 mV, it passed through the pore and the current signal returned to initial levels.

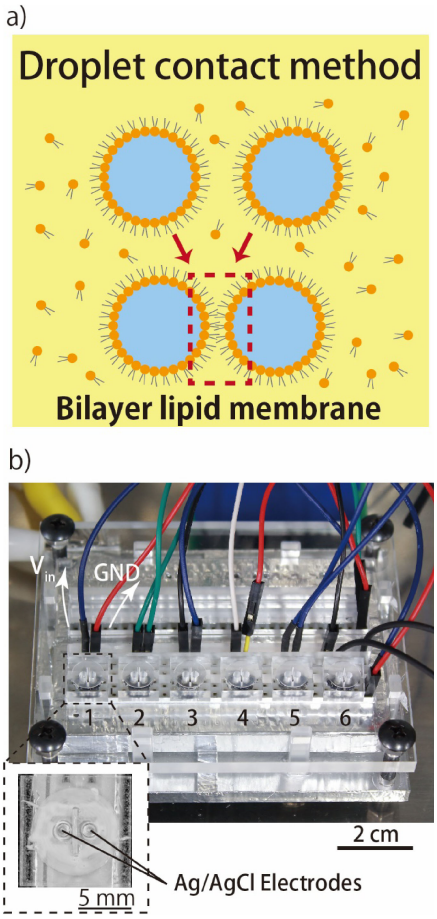

Figure 2. (Color online) a) A schematic illustration of the droplet contact method used for preparing a lipid bilayer. b) A photograph of the lipid bilayer array. This device has six chambers and is connected to multiple patch-clamp amplifiers.

designed the variable array device using commercially available breadboard in an attempt to reveal the relationship between the hybridization energy (ΔG) and the unzipping kinetics of hairpin DNA (hpDNA) using this device.

2. Experimental

2.1 Reagents and chemicals

In this study, we used the following reagents: 1,2-diphytanoyl-*sn*-glycero-3-phosphocholine (DPhPC; Avanti. Polar Lipids, AL, USA); *n*-decane (Wako Pure Chemical Industries, Ltd., Osaka, Japan); 3-morpholinopropane-1-sulfonic acid (MOPS, Nacalai Tesque, Kyoto, Japan); and potassium chloride (KCl; Nacalai Tesque). Buffered electrolyte solutions were prepared from ultrapure water, which was obtained from a Milli-Q system (Millipore, Billerica, MA, USA). αHL (Sigma–Aldrich, St. Louis, MO, USA) was obtained as a monomer protein isolated from *Staphylococcus aureus* in the form of a powder, and dissolved at a concentration of 1 mg/mL in ultrapure water and stored at −80°C. For use, samples were diluted to 0.5 μM using a buffered electrolyte solution and stored at 4°C. Hairpin DNA (FASMAC Co., Ltd., Kanagawa, Japan) was obtained from DNA synthesis in the form of a powder, and dissolved at a concentration of 100 μM in ultrapure water and stored at −20°C.

2.2 Design and formation of hairpin DNA

The free energy of the hpDNA was calculated from the thermodynamic simulation using the Nucleic Acid Package (NUPACK) software (http://www.nupack.org/).[19] In this simulation, when the stem of the double-strand of the hpDNA was increased, free energy also increased. Annealing of the folded strands was conducted by heating hpDNA samples for 5 min at 100 μM in ultrapure water to 95°C followed by rapid cooling to 4°C.

2.3 Preparation of multi-channel device

The multi-channel device was fabricated by machining a 6.0 mm thick, 10 × 10 mm polymethyl methacrylate (PMMA) plate (Mitsubishi Rayon, Tokyo, Japan) using a computer-aided design and/computer-aided manufacturing three dimensional modeling machine (MM-100, Modia Systems, Japan) as shown in Fig. 2b. Two wells (2.0 mm diameter and 5.0 mm depth) and a chase between the wells were manufactured on the PMMA plate. Each well had a through-hole in the bottom and Ag/AgCl electrodes set into this hole. A polymeric film made of parylene C (polychloro-*p*-xylylene) with a thickness of 5 μm was patterned with single pores (100 μm diameter.) using conventional photolithography method,[12] and then fixed between PMMA films (0.2 mm thick) using an adhesive bond (Super X, Cemedine Co., Ltd., Tokyo, Japan). The films, including the parylene film, were inserted into the chase to separate the wells. Ag/AgCl electrodes of each device were set to a solderless breadboard (E-Call Enterprise Co., Ltd., Taipei City, Taiwan), which was connected to a Jet patch-clamp amplifier (Tecella, Foothill Ranch, CA, USA) using jumper wire.

2.4 Bilayer lipid membrane preparation and reconstitution of α-hemolysin

Bilayer lipid membranes (BLMs) were prepared using an arrayed device, which had six chambers on the breadboard. Six individual BLMs can be simultaneously formed in this device, which allowed for a higher-throughput measurement compared to the conventional system. First, the DPhPC (lipids/*n*-decane, 10 mg/mL) solution (2.4 μL) was poured into all chambers. Next, the buffer solution (4.7 μL) without αHL and hpDNA was poured into each recording chamber. The buffer solution (4.7 μL) with αHL (final concentration 0.005 μM) and hpDNA (final concentration 10 μM) was poured into each ground chamber. In this study, the buffer solution (1 M KCl, 10 mM MOPS, pH 7.0) was used for all droplets. A few minutes after adding the buffer solution the two lipid monolayers connected and formed BLMs, and αHL formed nanopores by reconstitution in the BLMs. When the BLMs ruptured, we reformed the BLMs by tracing with a hydrophobic stick between two droplets.[18]

2.5 Channel current measurements and data analysis

Channel current was monitored using a Jet patch-clamp amplifier connected to each chamber. Ag/AgCl electrodes were already present in each droplet when we added the solution into the chambers. A constant voltage of +120 mV was applied to the recording chamber, and the ground chamber was grounded. Reconstituted αHL in BLMs allowed ions to pass through a nanopore under the voltage gradient, and we obtained the channel current signals. When hpDNA was present in the ground chamber the nanopore containing the αHL was blocked by this DNA and the channel current decreased. When hpDNA passed through the nanopore, the channel current increased. We defined those processes of electric current change as the duration time. The signals were detected using a 4 kHz low-pass filter at a sampling frequency of 20 kHz. Analysis of channel current signals and duration time was performed using pCLAMP ver. 10.5 (Molecular Devices, CA, USA) and Excel (Microsoft, Washington, USA) software. Signature events of hpDNA were obtained from more than 10% current blockades from an open current level in a single nanopore. Between 40 and 1300 unzipping events were recorded in this study. All data were presented as mean values ± SE, where each duration time was taken using the natural logarithm. Channel current measurements were conducted at 22 ± 2°C.

Table 1. The hairpin DNA sequences.

HP4	5′-AACGTTTTCGTTAAAAAAAAAAAAAAAAAA-3′	32	mer
HP6	5′-CGAACGTTTTCGTTCGAAAAAAAAAAAAAAAAAAAA-3′	36	mer
HP8	5′-GTCGAACGTTTTCGTTCGACAAAAAAAAAAAAAAAAAAAA-3′	40	mer
HP10	5′-CAGTCGAACGTTTTCGTTCGACTGAAAAAAAAAAAAAAAAAAAA-3′	44	mer
HP12	5′-CCCAGTCGAACGTTTTCGTTCGACTGGGAAAAAAAAAAAAAAAAAAAA-3′	48	mer
HP14	5′-AACCCAGTCGAACGTTTTCGTTCGACTGGGTTAAAAAAAAAAAAAAAAAAAA-3′	52	mer
HP16	5′-CGAACCCAGTCGAACGTTTTCGTTCGACTGGGTTCGAAAAAAAAAAAAAAAAAAAA-3′	56	mer

Table 2. The melting energy of each hairpin DNA calculated using NUPACK. (at 22°C)

Stem of hairpin (base-pair)	ΔG_{sim} (kJ mol^{-1})
4	−18.2
6	−38.5
8	−53.2
10	−66.9
12	−84.9
14	−95.2
16	−115.5

3. Results and Discussion

3.1 Channel current recordings of hairpin DNA by lipid bilayer array

We first designed the hpDNA sequence using thermodynamic simulation. Table 1 shows the hpDNA, which has 4 to 16 base pairs with a 20 adenine tail designed by NUPACK, and their melting free energy ($-\Delta G_{sim}$) is listed in Table 2. The absolute-value of free energy was gradually increased with increasing the lengths of the hairpin duplex. We next measured the unzipping time of the hpDNA in the αHL nanopore. The typical current and time traces of each hpDNA (HP6 to HP12) are shown in Fig. 3. We considered in this paper that there are two consecutive steps in the nanopore unzipping process: i) the hairpin region of dsDNA are clogged in the vestibule following the entry and sliding of the ssDNA tail in the pore; ii) the hairpin region is unzipped and the unzipped single-stranded DNA translocates through the nanopore. These two steps can be observed in the channel current signals. We defined the blocking time of hpDNA as the duration time (t) in the subsequent experiments.

3.2 The length dependency of the complementary strand of hairpin DNA on the unzipping behavior

Figure 4a shows the duration time, t, as a function of ΔG_{sim} calculated from thermodynamic simulation. Although we expected the duration time to initially scale linearly with the free energy, t increased with increasing ΔG_{sim} logarithmically in this experiment. It has been previously argued that the unzipping kinetics of dsDNA can be exhibited in first-order reactions.[6] It is well known that the first-ordered dissociation of enzyme reaction is described as Michaelis-Menten model. This reaction can be represented schematically as below.

$$[E] + [S] \rightleftarrows [ES] \rightarrow [E] + [P]$$

where E is enzyme, S is substrate, ES is complex with enzyme and substrate, and P is product. Thus, in this paper, we considered this

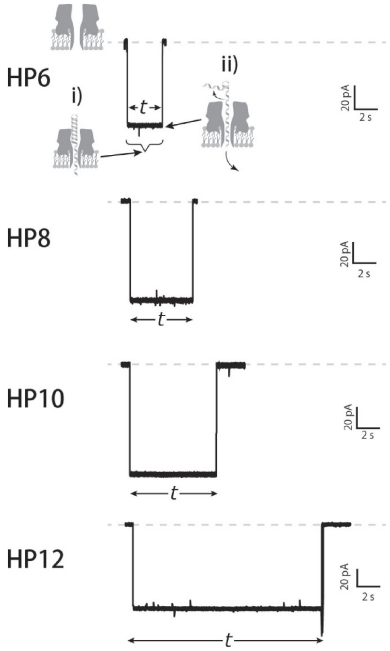

Figure 3. The typical current and time traces of hairpin DNA unzipping in the nanopore.

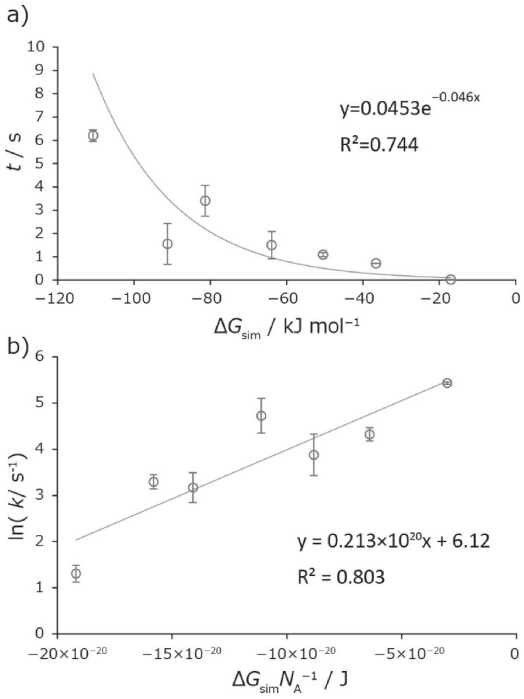

Figure 4. a) Duration time of hpDNA as a function of hybridization energy calculated using NUPACK. b) The relationship between the first order rate constant and the hybridization energy. The plots were fitted using the Eq. (1).

unzipping behavior as the first-ordered dissociation reaction, and it can be described as following.

$$[\text{hpDNA} + \alpha\text{HL}] \rightarrow [\text{ssDNA}] + [\alpha\text{HL}]$$

The rate constant of this reaction can be described as below.

$$k = k_0 \exp(-\Delta G_{\text{sim}}/N_{\text{A}}k_{\text{B}}T) \quad (1)$$

$$k = 1/t$$

where k is the dissociation rate constant, k_0 is the initial rate constant, N_{A} is the Avogadro constant, k_{B} is Boltzmann constant used for this single molecule experiment instead of a gas constant, and T is temperature. The k (s^{-1}) should be equal to the inverse of t because $1/t$ is the reaction frequency per unit of time at the single molecule reaction. Figure 4b shows the plot of k as a function of ΔG_{sim}. The plots were well fitted using the Eq. (1), indicating the inverse value of the duration time is as the first-order rate constant. This result can be used for the prediction of unzipping time using the simulated free energy. The unzipping time of dsDNA is occasionally required in the nanopore/DNA experiments. Therefore, this prediction will be useful for DNA or RNA deign in the extended nanopore study and also be useful for understanding of DNA related biological reactions.

4. Conclusion

In summary, we examined hpDNA unzipping time using an αHL nanopore by changing the length of the complementary region of the hpDNA from 4 to 16 bases. The hpDNA was initially obstructed in the nanopore, and thus it was unzipped and electrophoretically passed through the nanopore. The duration time of captured hpDNA had a logarithmic relation with the melting free energy ($-\Delta G_{\text{sim}}$) of hpDNA estimated from thermodynamic simulation. Therefore, we modeled it as a first-order dissociation reaction, and fitted the data using the kinetic equation. Our study will be useful for the design of dsDNA, to be able to determine their blocking time in the nanopore. Moreover, the high-throughput nanopore measurement described here will be applied to analysis of extensive biological reactions, such as the binding of transcription factors to dsDNA and the movement of enzymes along the length of a DNA chain.

Acknowledgment

This work was partly supported by a Grant-in-Aid for Scientific Research on Innovative Areas (No. 24104002) and Scientific Research No. 26540160 and 25708024 of The Ministry of Education, Culture, Sports, Science and Technology, and Global Innovation Research Organization in TUAT.

References

1. L. Q. Gu, O. Braha, S. Conlan, S. Cheley, and H. Bayley, *Nature*, **398**, 686 (1999).
2. J. J. Kasianowicz, E. Brandin, D. Branton, and D. W. Deamer, *Proc. Natl. Acad. Sci. U.S.A.*, **93**, 13770 (1996).
3. S. M. Bezrukov, I. Vodyanoy, and V. A. Parsegian, *Nature*, **370**, 279 (1994).
4. X. F. Kang, S. Cheley, X. Y. Guan, and H. Bayley, *J. Am. Chem. Soc.*, **128**, 10684 (2006).
5. J. Nivala, D. B. Marks, and M. Akeson, *Nat. Biotechnol.*, **31**, 247 (2013).
6. A. F. Sauer-Budge, J. A. Nyamwanda, D. K. Lubensky, and D. Branton, *Phys. Rev. Lett.*, **90**, 238101 (2003).
7. D. Branton, D. W. Deamer, A. Marziali, H. Bayley, S. A. Benner, T. Butler, M. Di Ventra, S. Garaj, A. Hibbs, X. H. Huang, S. B. Jovanovich, P. S. Krstic, S. Lindsay, X. S. S. Ling, C. H. Mastrangelo, A. Meller, J. S. Oliver, Y. V. Pershin, J. M. Ramsey, R. Riehn, G. V. Soni, V. Tabard-Cossa, M. Wanunu, M. Wiggin, and J. A. Schloss, *Nat. Biotechnol.*, **26**, 1146 (2008).
8. J. Liphardt, B. Onoa, S. B. Smith, I. Tinoco, and C. Bustamante, *Science*, **292**, 733 (2001).
9. J. Mathe, H. Visram, V. Viasnoff, Y. Rabin, and A. Meller, *Biophys. J.*, **87**, 3205 (2004).
10. O. K. Dudko, J. Mathe, A. Szabo, A. Meller, and G. Hummer, *Biophys. J.*, **92**, 4188 (2007).
11. Y. Ding, A. M. Fleming, H. S. White, and C. J. Burrows, *J. Phys. Chem. B*, **118**, 12873 (2014).
12. R. Kawano, T. Osaki, H. Sasaki, and S. Takeuchi, *Small*, **6**, 2100 (2010).
13. R. Kawano, Y. Tsuji, K. Sato, T. Osaki, K. Kamiya, M. Hirano, T. Ide, N. Miki, and S. Takeuchi, *Sci. Rep.*, **3**, 1995 (2013).
14. R. Kawano, T. Osaki, H. Sasaki, M. Takinoue, S. Yoshizawa, and S. Takeuchi, *J. Am. Chem. Soc.*, **133**, 8474 (2011).
15. Y. Tsuji, R. Kawano, T. Osaki, K. Kamiya, N. Miki, and S. Takeuchi, *Anal. Chem.*, **85**, 10913 (2013).
16. H. Watanabe and R. Kawano, *Anal. Sci.*, **32**, 57 (2016).
17. Y. Tsuji, R. Kawano, T. Osaki, K. Kamiya, N. Miki, and S. Takeuchi, *Lab Chip*, **13**, 1476 (2013).
18. R. Kawano, Y. Tsuji, K. Kamiya, T. Kodama, T. Osaki, N. Miki, and S. Takeuchi, *PLoS ONE*, **9**, e102427 (2014).
19. R. M. Dirks, J. S. Bois, J. M. Schaeffer, E. Winfree, and N. A. Pierce, *Siam Review*, **49**, 65 (2007).